Atmospheric Environment 47 (2012) 66–75

Contents lists available at SciVerse ScienceDirect

Atmospheric Environment

journal homepage: www.elsevier.com/locate/atmosenv

An inventory of global N_2O emissions from the soils of natural terrestrial ecosystems

Qianlai Zhuang [a,b,*,1], Yanyu Lu [a,b,c,**,1], Min Chen [a]

[a] Department of Earth & Atmospheric Sciences, Purdue University, West Lafayette, IN, USA
[b] Department of Agronomy, Purdue University, West Lafayette, IN, USA
[c] AnHui Climate Center, Hefei, China

ARTICLE INFO

Article history:
Received 19 July 2011
Received in revised form
14 October 2011
Accepted 16 November 2011

Keywords:
Global N_2O emissions
Artificial neural network
Ecosystems
Greenhouse gas

ABSTRACT

We develop an inventory of global N_2O emissions from natural ecosystem soils using an artificial neural network approach and field observational data of N_2O fluxes. We estimate that the global soil N_2O source strength from natural ecosystems is 3.37 Tg (1 Tg = 10^{12} g) N per year with an uncertainty ranging from 1.96 to 4.56 Tg N per year in 2000. While our global estimate is lower than other existing estimates, the spatial patterns of our simulated N_2O emissions agree with other existing studies. There was a large spatial and seasonal variability in the soil N_2O emissions due to the variation in soil type, vegetation and climate conditions. Consistent with other studies, we confirm that warm and moist tropical soils are the major source of atmospheric N_2O. As a result of the low temperatures, the high latitude ecosystems have significantly low emission rates and contribute little (less than 0.10 Tg N per year) to the global N_2O source. The simulated annual global N_2O emissions are found to be most sensitive to variation in precipitation. This study uses the most current available data for N_2O fluxes and their associated environmental variables to quantify the global N_2O emissions, and provides an independent global inventory of this important trace gas, which will facilitate future studies of atmospheric chemistry and climate feedbacks at the global scale.

1. Introduction

Atmospheric nitrous oxide (N_2O) is one of the most important trace gases, contributing 0.16 Wm^{-2} of radiative forcing to global warming. On a molar basis, its global warming potential is about 296 times that of CO_2 on a 100-year time horizon (IPCC, 2007). The reaction of N_2O with oxygen atoms plays an important role in stratosphere ozone depletion, producing NO, which in turn reacts with ozone. The atmospheric concentration of N_2O has increased from 270 ppb in preindustrial times to the current level of 319 ppb. N_2O is mainly of biogenic origin. The soils of natural ecosystems have been recognized as one major source of N_2O. Currently, soils of natural ecosystems are considered to emit 6.6 Tg N yr^{-1} of N_2O, which is about 37% of the total global surface emissions (IPCC, 2007). This reported soil emission rate is based on a single model estimate from Bouwman et al. (1995). However, to date, there are more available data from laboratory experiments and field measurements. In addition, the mechanistic understanding of the processes and controls of soil N_2O emissions have also advanced. Thus, current emission estimates should be revised to take advantage of the available data and knowledge.

N_2O emissions from soils are produced predominantly by the microbial processes of nitrification and denitrification, while denitrification is also a sink for N_2O (Conrad, 1996; Smith and Conen, 2004). The factors controlling N_2O emissions have been extensively reviewed (e.g., Skiba and Smith, 2000; Bouwman et al., 2002a). Owing to the improved knowledge of the processes and factors responsible for N_2O emissions, the bottom-up approaches, including process-based models (e.g., Li et al., 1992; Parton et al., 1996; Butterbach-Bahl et al., 2009) and empirical methods (e.g., Bouwman, 1996; Bouwman et al., 2002b; Flynn et al., 2005), have been used extensively to estimate N_2O emissions from agricultural soils at site, regional, and global scales. In contrast with the extensive studies on emissions from agricultural soils, less effort has been made on the estimation of emissions from soils under natural vegetation. Stehfest and Bouwman (2006) summarized the

* Corresponding author. Department of Earth & Atmospheric Sciences, Purdue University, CIVIL 550 Stadium Mall Drive, West Lafayette, IN 47907-2051, USA. Tel.: +1 765 494 9610; fax: +1 765 496 1210.
** Corresponding author. Department of Earth & Atmospheric Sciences, Purdue University, West Lafayette, IN, USA.
E-mail addresses: qzhuang@purdue.edu (Q. Zhuang), lu26@purdue.edu (Y. Lu).
[1] These authors equally contributed to the study.

1352-2310/$ – see front matter © 2011 Elsevier Ltd. All rights reserved.
doi:10.1016/j.atmosenv.2011.11.036

published field measurement data and developed a statistical emission model for soils under natural vegetation, but they did not provide an estimate at the global scale due to lack of data. More recently, Werner et al. (2007a) estimated the total N_2O source strength of 1.34 Tg N yr^{-1} with an uncertainty range of 0.88–2.37 Tg N yr^{-1} from the global tropical rainforest soils using a biogeochemical model, the DeNitrification–DeComposition (DNDC) model. To our knowledge, there is a gap in the development of a global inventory of N_2O emissions from the soils of natural ecosystems. In this study we attempt to fill in this gap using an Artificial Neural Network (ANN) approach as well as the available observational data of N_2O fluxes.

The ANN approach has appeared as a great alternative to classical statistical modeling in many disciplines (e.g., Anghel and Ozunu, 2006; Delon et al., 2007; Dupont et al., 2008). It is particularly useful in quantifying the responses of non-linear processes like soil N_2O emissions, which are determined by numerous direct and indirect factors. In this study, we first use the ANN approach to find the best non-linear regression between key environmental factors and N_2O emission fluxes. Driven with spatially-explicit data of monthly climate, soils, and topography, the developed ANN is then extrapolated to the global terrestrial ecosystem to develop a global soil N_2O emission inventory.

2. Methods

2.1. Data organization

To begin, we collect direct N_2O measurements of various terrestrial ecosystems from peer-reviewed literature (e.g., Wang et al., 2003; Mo et al., 2006; Stehfest and Bouwman, 2006). Our data contain 209 records for natural ecosystems at 64 sites (Table 1). The observed sites cover a range of ecosystem types including forests, savannas, shrublands, and grasslands under various field conditions related to climate, soils, site management and measurement techniques. The emissions are recorded as the sum of emissions over a measurement period, which ranges from a few days to several years. If the measurements cover more than a one-year period, the emission values are then averaged to get single-year values at a monthly time step.

To generate a complete dataset covering various ecosystem types, we retrieve climate and soil property information from the original literature. Specifically, climate information is derived from a historical climate database from the Climate Research Unit (CRU) (Mitchell and Jones, 2005). Soil organic carbon and nitrogen and bulk density in the top soil (0–30 cm) are taken from the World Inventory of Soil Emission Potentials (ISRIC-WISE) spatial soil database (Batjes, 2006). Based on the geographic coordinates and experiment date of the measurement retrieved from the original research papers, we compile the data of precipitation (P), mean air temperature (T) of the experiment periods, soil organic carbon (SOC), soil nitrogen content (SN), and bulk density (BD) for all experiment sites used in this study.

2.2. Neural network development

We adapt a General Regression Neural Network (GRNN) algorithm (Specht, 1991) to represent non-linear mapping between the independent variables and dependent variable. GRNN approximates any arbitrary function between the input and output vectors of these independent and dependent variables, drawing the function estimate directly from the training data (Cigizoglu and Alp, 2006). As the number of training samples increases, the GRNN asymptotically converges to the optimal regression surface and the estimation error approaches zero, with only mild restrictions on the function. Generally, the GRNN has a four-layer architecture consisting of an input layer, a hidden layer, a summation layer, and a decision layer (Fig. 1; Delon et al., 2007; Cigizoglu and Alp, 2006). In the input layer, there is one neuron for each independent variable. Here, a neuron is defined as a mathematical function in an artificial neural network. The input neurons standardize the range of the independent variable values. These input neurons then transfer the values to the neurons in the hidden layer. Each neuron in the hidden layer stores the values of the independent variables and the dependent variable and calculates a scalar function that will be used in the summation layer. The first neuron in the summation layer is the denominator summation unit, which sums the weight values coming from the hidden neurons. The second neuron of this layer is the numerator summation unit, which sums the weight values multiplied by the actual target dependent variable value for each hidden neuron. Finally, the decision layer divides the value accumulated in the numerator summation unit by the value in the denominator summation unit and uses the result as the predicted target dependent variable value (e.g., Disorntetiwat and Dagli, 2000).

Before developing a neural network, all training data for the independent and dependent variables are standardized such that all data have the same order of magnitudes in the input layer. The training dataset includes an independent variable vector x (e.g., monthly air temperature) and a dependent variable vector (monthly N_2O emission fluxes). In the hidden layer, the scalar function $D_i^2 = (x - x_i)^T(x - x_i)$ is used to provide values for the summation layer. x_i denotes the ith training independent vector x (e.g., air temperature). The predicted target dependent variable, the N_2O fluxes, is defined:

$$y' = \frac{\sum_{i=1}^{n} y_i \exp\left(-D_i^2/2\sigma^2\right)}{\sum_{i=1}^{n} \exp\left(-D_i^2/2\sigma^2\right)} \quad (1)$$

Where the values calculated with the scalar function in a hidden neuron i are weighted with the corresponding values of the training samples y_i, and then passed to the numerator neuron. n is the number of sample observations. σ is the spread parameter, whose optimal value is determined by minimizing the root mean square error (RMSE) between the training data and the predicted values of the dependent variable. The weight of the denominator neuron is set to 1.0. The GRNN training algorithm uses only one adjustable parameter σ for a given training set. The magnitude of σ affects the accuracy of GRNN. Here we use "the holdout method" (Specht, 1991) to optimize the σ value. This technique removes one input–output vector from the training set to build a GRNN model, and uses the remaining vectors to predict the outputs corresponding to the removed vector. Repeating the "removing" process for each sample and storing each estimate of GRNN, the mean-squared error (MSE) between the GRNN-predicted and the corresponding sample values is calculated. The procedure is repeated by varying the σ value, and the value that minimized the MSE is chosen for the final ANN. MATLAB codes are used in the development of the ANN model (The Mathworks, 2006).

2.3. Global extrapolation

To extrapolate the final ANN model to the global natural ecosystem at a monthly time step, we organize the spatially-explicit data of climate, soil properties, and vegetation. The climate data including monthly mean air temperature and monthly precipitation at a $0.5^\circ \times 0.5^\circ$ resolution are from climate model simulations from the Climate Research Unit (CRU) (Mitchell and Jones, 2005). The spatially-explicit soil organic carbon and

Table 1
Description of the sites used in this analysis.

Site name	Ecosystem type	*n*	Longitude (°)	Latitude (°)	Temperature (°C)	Precipitation (mm)	Carbon content (%)	Nitrogen content (%)	Bulk density (g cm^{-3})	Length of experiment	N_2O flux (kg N ha^{-1} yr^{-1} or per measurement period)	Reference
San Dimas, California	Savanna	1	−118	34	14.8	148.6	0.82	0.1	1.34	180	0.00	Anderson and Poth (1989)
Harvard forest, Massachusetts, USA	Coniferous	2	−72.5	41.5	10.1	902	2.76	0.22	0.87–1.32	360	0.01–0.02	Bowden et al. (1990)
Kauri Creek, Australia	Rainforest	4	145.5	−17.5	17.6–23.9	25.5–252.3	3.2	0.22	1.05	10–19	0.03–0.35	Breuer et al. (2000)
Lake Eacham, Australia	Rainforest	4	145.5	−17	20.2–27.1	42.2–309.3	2.34	0.15	0.99	8–22	0.02–0.09	Breuer et al. (2000)
Massey Creek, Australia	Rainforest	3	145.5	−17.5	19.0–24.3	69.7–236.1	5.2	0.37	0.69	10–18	0.07–0.20	Breuer et al. (2000)
Höglwald, Germany	Coniferous	7	14	51	14.6	66.8	1.37	0.12	1.2	30	0.04–0.12	Butterbach-Bahl et al. (1997)
Ballyhooly, Republic of Ireland	Coniferous	4	−8.5	52	9.6	89.9	3.12	0.19	1.3	3	0.00	Butterbach-Bahl et al. (1998)
Mt. Ascutney, VT, USA	Coniferous	1	−72.5	43.5	18.7	366.9	3.96	0.25	1.22	120	−0.03	Castro et al. (1993)
Mt. Washington, NH, USA	Coniferous	1	−71	44.5	16.0	542.1	2.35	0.19	1.27	120	−0.01	Castro et al. (1993)
Mt. Mansfield, VT, USA	Coniferous	1	−73	44.5	17.0	422.1	2	0.14	0.87	120	0.06	Castro et al. (1993)
Whiteface Mt., NY, USA	Coniferous	1	−74	44.5	18.0	3.0	2.75	0.21	1.33	120	0.06	Castro et al. (1993)
Acadia, ME, USA	Coniferous	1	−68.5	44.5	18.1	299.4	3.17	0.23	1.32	120	0.01	Castro et al. (1993)
Baraboo	Grass	3	−89.5	43.5	11.5	232–274	0.9–2.4	0.08	1.24	240	0.03–0.04	Cates and Keeney (1987)
Everglades, Florida, USA	Marsh	1	−80.5	26	24.0	1449.6	30.08	2.26	1.34	360	1.00	Duxbury et al. (1982)
New York, USA	Deciduous	1	−76.5	42.5	7.6	916.8	0.8	0.08	1.38	360	0.90	Duxbury et al. (1982)
Guánica Commonwealth Forest, SW Puerto Rico	Tropical dry forest	4	−66	18	25.4	1724.4	5.07–7.88	0.49–0.80	0.79–1.01	330	0.02–0.7	Erickson et al. (2002)
Fazenda Nova Vida, Rondônia, Brazil	Rainforest	3	−63	−10	25.6–26.3	108.4 −1626.4	1.03	0.09	1.05	153–365	0.5–3.22	Garcia-Montiel et al. (2003)
Lake Wingra Basin, Wisconsin, USA	Marsh	4	−89.5	43.5	18.5	651.5	6.4–32.6	0.38–3.07	0.29–1.38	105–210	0.02–7.40	Goodroad and Keeney (1984)
Lake Wingra Basin, Wisconsin, USA	Grass	6	−89.5	43.5	18.5	651.5	6.5–15.6	0.51–1.30	0.39–1.17	147–184	0.09–1.40	Goodroad and Keeney (1984)
Lake Wingra Basin, Wisconsin, USA	Coniferous	4	−89.5	43.5	18.5	651.5	2.4–2.6	0.15–0.19	1.15–1.18	147–231	0.19–2.10	Goodroad and Keeney (1984)
Poppel, Belgium	Deciduous	2	5	51.5	11.0	657–1017.6	7.8	0.3	0.73	317–365	0.00	Goossens et al. (2001)
Chaguarama, Guarico State, Venezuela	Savanna	2	−79.5	36.5	3.5	104.8	1.20–1.25	0.13–0.14	1.29	9	0.01	Hao et al. (1988)
10 km from Chaguarama, Guarico State, Venezuela	Savanna	2	−79.5	36.5	3.5	104.8	1.2	0.13–0.14	1.32–1.34	9	0.03	Hao et al. (1988)
Lake Creek, Linn County, Willamette valley, Oregon	Grass	2	−123.5	44.5	10.7	305.7	2.74–2.77	0.23–0.24	1.1–1.3	93	0.31	Horwath et al. (1998)
Jambi forest, Sumatra, Indonesia	Rainforest	5	102	−1	27.5	2217.6	1.6–4.5	0.12–0.65	0.81–1.20	365	0.07–0.69	Ishizuka et al. (2002)
La Selva Biological Station, Sarapiqui Canton, Costa Rica	Rainforest	2	−83.5	9.5	24.9	3225.6	3	0.47–0.60	0.62–0.64	365	3.74–5.86	Keller and Reiners (1994)
Manaus, Brazil	Rainforest	6	−60	−3	25–28	206.2–326.4	1	0.08	1.14–1.38	30	0.09–0.80	Keller et al. (1983)
Tena, Ecuador	Rainforest	2	−77.5	−1	22.0	2.4	2.84	0.2	1.34	30	0.05	Keller et al. (1986)
Puerto Rico	Tropical dry forest	4	−66	18	19.0–30.0	37.9	1.23	0.11	1.33–1.42	30	0.02–0.30	Keller et al. (1986)
Hubbard Brook, New Hampshire, USA	Deciduous	1	−71.5	44	3.2	1501.2	4.34	0.27	0.87	365	0.90	Keller et al. (1983)
Ducke Reserve, INPA, Brazil	Rainforest	1	−60	3	25.0	369.3	0.92	0.09	1.22	28	0.16	Keller et al. (1988)
Kauri Creek, Queensland, Australia	Rainforest	3	145.5	−17.5	23.7	677–3138	3.2	0.22	1.05	55–365	0.38–4.36	Kiese and Butterbach-Bahl (2002)
Pin Gin Hill, Queensland, Australia	Rainforest	3	146	−17.5	21.3–23.7	677–3138	9.15	0.66	0.79	55–365	0.33–6.89	Kiese and Butterbach-Bahl (2002)
Bellender Ker, Queensland, Australia	Rainforest	3	146	−17.5	21.3	677–3138	3.1	0.26	1.09	55–365	1.33–7.45	Kiese and Butterbach-Bahl (2002)
Kruger Park, South Africa	Savanna	2	22.5	−31	25.0	0.1	1.9–2.5	0.05–0.09	1.6	13–15	0.01	Levine et al. (1996)
Manaus, Brazil	Rainforest	5	−60	−3	27.8	75.6–2018.4	1	0.07–0.22	0.87–1.34	11–365	0.03–2.2	Luizão et al. (1989)
La Selva Biological Station, Sarapiqui Canton, Costa Rica	Rainforest	3	−83.5	9.5	25.0	227.1	2.25	0.19	0.87–1.05	10	0.04–0.06	Matson and Vitousek (1987)

Turrialba, Costa Rica	Rainforest	1	−83.5	10	22.0	184	2.02	0.16	1.46	10	0.04	Matson and Vitousek (1987)
Hawaii	Rainforest	3	−84	10.5	16.0	332.8	1.03	0.09	1.32−1.39	10	0.00	Matson and Vitousek (1987)
Manaus, Brazil	Rainforest	5	−60	−3	28.1	102.7	1.6−8.4	0.08−0.26	0.87−1.38	45	0.01−1.08	Matson et al. (1990)
Fazenda Nova Vida, Rondônia, Brazil	Rainforest	1	−63	−10	26.0	2228.4	1.03	0.09	1.39	365	1.94	Melillo et al. (2001)
Kiel, Germany	Deciduous	2	10	54	8.4	735.6	3.4−42	0.2−2.4	0.6−1.1	365	0.4−4.9	Mogge et al. (1998)
Dinghu Mountain, Guangdong, China	Coniferous	3	112.5	23	21.4	1927	1.58−3.1	0.09−0.19	1.21−1.41	365	1.86−5.18	Mo et al. (2006)
Colorado, USA	Grass	1	−105	39.5	17.8	249	1.4	0.13	1.32	62	0.14	Mosier et al. (1981)
US Dept. Energy Hanford site, South-Central Washington	Grass	1	−120.5	47	8.6	313.2	2.66	0.24	1.34	365	0.15	Mummey et al. (1997)
Yurimaguas, Loreto Province, Peru	Rainforest	2	−76	−6	26	2200	1.1	0.08	1.25−1.41	365	0.80	Palm et al. (2002)
Ft. Collins, Colorado, USA	Grass	2	−104.5	38.5	10.6	476.4	0.57	0.07	1.32−1.34	365	0.08−0.16	Parton et al. (1988)
Central Scotland	Deciduous	3	−4.5	56.5	8.7	828.8	14.35	0.01	1.22−1.32	210	1.15−2.29	Pitcairn et al. (2002)
Brasilia, Brazil	Savanna	3	−48	−16	25.0	108.3	5.18−6.06	0.26−0.32	1.08−1.33	1	0.00	Poth et al. (1995)
Molokai, Hawaii	Rainforest	1	−155	19.5	15.9	2500	8.9	0.49	1.33	365	0.16	Riley and Vitousek (1995)
Kauai, Kokee State forest, Hawaii	Rainforest	1	−155.5	20	16.1	2410	3.99	0.05	1.22	365	0.26	Riley and Vitousek (1995)
Kohala, Hawaii	Rainforest	1	−155.5	20	16.1	2540	3.99	0.05	1.38	365	0.39	Riley and Vitousek (1995)
Kilauea, Hawaii	Rainforest	1	−157	21	16.1	2410	4.24	0.01	1.29	365	0.02	Riley and Vitousek (1995)
Puu Makaala, Hawaii	Rainforest	1	−159.5	22	16.6	3800	1.7	0.07	1.35	365	0.23	Riley and Vitousek (1995)
Guri Dam, Bolivar State, Venezuela	Savanna	4	−63	8	27.5	150	1.09−3.50	0.08−0.13	0.87−1.35	20	0.01−0.12	Sanhueza et al. (1990)
Estanción Biológica de los Llanos, Calabozo, Guárice state	Savanna	1	−67.5	9	30.0	75.5	0.9	0.08	1.29	19	0.03	Sanhueza et al. (1994)
Langenlonsheim, Bingen, Germany	Deciduous	2	7.5	49.5	9.1	808.8	2.8−7.2	0.21−0.29	1.33	360	0.67−0.73	Schmidt et al. (1988)
Bechenheim, Alzey, Germany	Deciduous	2	8	49.5	11.0	697.2	2.4−3.4	0.11−0.18	1.33−1.35	360	0.67−0.92	Schmidt et al. (1988)
Ober-Olm, Mainz, Germany	Deciduous	2	8	50	8.6	823.2	2.8−3.6	0.16−0.30	1.08−1.32	360	0.26−0.33	Schmidt et al. (1988)
Nylsvley Reserve, South Africa	Savanna	2	28.5	−24.5	28.8	48.9	1.09−1.42	0.06−0.16	1.34−1.35	10	0.02	Scholes et al. (1997)
Mainz, Germany	Grass	3	8.5	50	10.0	45.5−546	0.8−2.3	0.12	1.32−1.38	32−71	0.02−0.13	Seiler and Conrad (1981)
Mayombe, Congo	Rainforest	3	12.5	−4	22.4−26.6	0−135.6	3.5	0.23	0.97−1.34	1	0−0.05	Serca et al. (1994)
Dunslair Heights, NW England	Coniferous	3	−2.5	54.5	7.5	1143.6	4.52	0.24	1.31−1.39	240	0.06−0.22	Skiba et al. (1997)
Bush Estate, Edinburgh	Deciduous	2	−3	56	13.8	202	1.09	0.1	1.22−1.38	120	0.09−0.15	Skiba et al. (1997)
Devilla forest, Central Scotland	Coniferous	2	−4	57	5.4	1015.2	9.27	0.44	1.21−1.36	180−330	0.23−0.26	Skiba et al. (1997)
South Scotland	Grass	3	11.5	55.5	18.2	26.7	1.72	0.15	1.29−1.37	3	0.00	Skiba et al. (1998)
Central Scotland	Grass	4	−4.5	56.5	12.6	129.3	14.35	0.66	0.87−1.38	7	0.02−0.09	Skiba et al. (1998)
Central Scotland	Mixed forest	13	−4.5	56.5	8.4	953.4	14.35	0.66	0.87−1.48	150−210	0−0.25	Skiba et al. (1999)
Barataria Basin, Louisiana, USA	Marsh	4	−91.5	29.5	19.9	1509.6	20.47	1.55	0.10−0.28	360	0.31−0.55	Smith et al. (1983)
Fazenda Nova Vida, Rondônia, Brazil	Rainforest	1	−63	−10	25.6	183	1.03	0.09	1.37	1	0.01	Steudler et al. (2002)
Paragominas, Pará State, Brazil	Grass	3	−47.5	−3	27.0	2377−2730	2.63	0.26	0.96	151−365	0−0.07	Verchot et al. (2006)
Paragominas, Pará State, Brazil	Rainforest	6	−47.5	−3	27.0	2377−2730	2.47−2.9	0.22−0.26	0.96−0.99	151−365	0.35−2.43	Verchot et al. (2006)
Chamela, Jalisco State, Mexico	Tropical dry forest	3	−105	19.5	25.1	341.9	1.4	0.15	1.32−1.37	30	0.01−0.19	Vitousek et al. (1989)
Island of Molokai, Kamakou Preserve, Hawaii	Tropical dry forest	3	−157	21	19−22	58.3−100	4.24	0.29	1.33−1.38	30	0.02−0.07	Vitousek et al. (1989)
Xilin River basin, Inner Mongolia, China	Grass	5	1.6	44	1.0	250−480	1.85	0.19	1.32	365	0.39−2.55	Wang et al. (2003)
La Selva Biological Station, Costa Rica	Rainforest	2	−83.5	9.5	22.9	3372	7.3−7.6	0.4	0.66−0.77	365	1.28−1.42	Weitz et al. (1998)

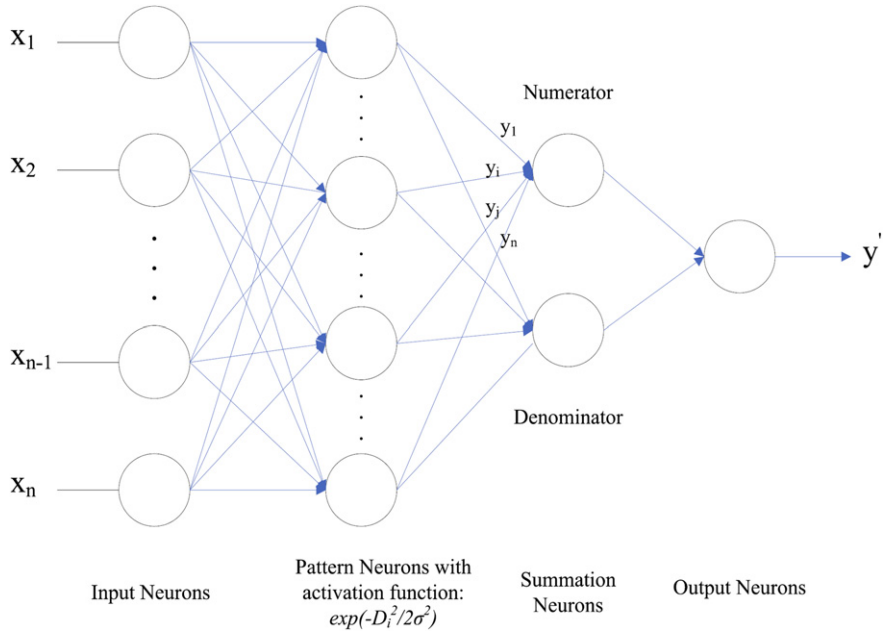

Fig. 1. Schematic diagram of the generalized regression neural network architecture based on Cigizoglu and Alp (2006).

nitrogen and bulk density in the top soil (0–30 cm) are taken from the spatial soil database of the World Inventory of Soil Emission Potentials (ISRIC-WISE) (Batjes, 2006). The ISRIC-WISE data are resampled to a resolution of 0.5° × 0.5°. The vegetation type and area data are derived from the combined land cover product of the Moderate Resolution Imaging Spectroradiometer (MODIS) on board Terra and Aqua (Land Cover Types Yearly L3 Global 0.05° CMG, MCD12C1, Year 2001) from the NASA Goddard Space Flight Center website (http://modis-land.gsfc.nasa.gov). The International Geosphere and Biosphere (IGBP) land-cover classification system is used to extract the vegetation type and area information.

To estimate global emissions of N_2O from natural ecosystem soils, we first run the ANN model to estimate monthly N_2O emission rates for each grid cell in 2000. Based on the simulated N_2O emission rates and the vegetation type and area data, we calculate the emissions for each grid cell, and then generate the global inventory.

2.4. Model sensitivity

To assess the sensitivity of the obtained ANN model, we conduct thirty other global simulations, altering climate and soil input parameters uniformly for each grid cell at the global scale. The input data of *P*, SOC, SN and BD are changed at three levels (small: ±10%, medium: ±25%, large: ±50%), while *T* is altered by ±1.0, ±2.5, and ±5.0 °C, respectively. Each variable is individually increased or decreased at the three levels. In each of these sensitivity simulations, when a single variable is changed, the other variables are held as same as they are in the "baseline" simulation that is driven with the unchanged global input data. The sensitivity is then calculated as the percentage change between the estimated annual emissions of each sensitivity simulation and the "baseline" simulation.

2.5. Uncertainty analysis

A regional or global inventory of soil N_2O emissions would typically have a wide range of emission estimates. The uncertainty in these inventories is mainly due to uncertain model structure and input data (IPCC, 2007). In our study, the uncertainty induced by input data can be revealed through sensitivity analysis. Here, we are mostly concerned with the uncertainty induced from the developed ANN model. Since the ANN is a highly non-linear system, and only provides the optimized value of weights, it is difficult to directly quantify the uncertainty range of the model through parametric inference. The model uncertainty is thus assessed through developing a number of alternative models using the delete-one cross-validation approach (Zhuang et al., 2008). Specifically, we randomly sample 150 data points from the organized measurement data. These samples are used to develop a new ANN model. The new model is then scaled up to obtain a new estimate of global emissions. These steps are repeated one hundred times to obtain one hundred sets of global estimates. The 95% confidence intervals of all estimates of N_2O emissions are considered to be the range of model uncertainty, and are thus applied to the final inventory calculations to define the lower and upper uncertainty bounds of the global N_2O inventory.

3. Results and discussion

3.1. Artificial neural networks

Before developing the ANN, we first conducted a Spearman rank correlation analysis to identify the key environmental factors for N_2O emissions using the measured flux data and organized independent variable data. The pair-wise correlation showed that soil N_2O emissions are significantly correlated with climate, soil properties, and the length of experiments (Table 2). Precipitation is the most important control for soil N_2O emissions. The high correlation between precipitation and N_2O flux is consistent with field observations, suggesting that water availability strongly constrains soil

Table 2
Spearman correlations between different factors and N_2O fluxes at the observational sites.

Parameter	*T*	*P*	SOC	SN	BD	Length of exp.
Coefficient	0.09	0.45	0.25	0.32	−0.32	0.38
p-value	0.18	<0.001	<0.001	<0.001	<0.001	<0.001

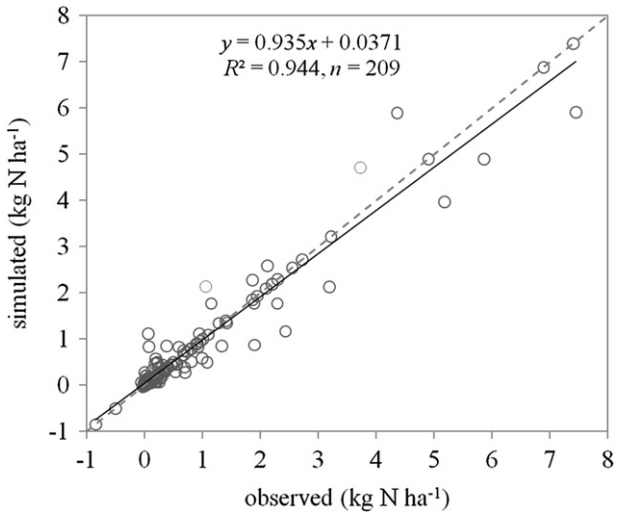

Fig. 2. Comparisons between the measured and modeled N_2O emissions. Dashed line is the 1:1 line.

nitrification and denitrification processes (Lu et al., 2006). Investigation at the site level indicates that temperature governs the seasonal variation in N_2O fluxes (Skiba and Smith, 2000). However, our analysis showed that temperature is only weakly correlated with N_2O fluxes across different sites, suggesting that temperature may not linearly affect soil N_2O emissions. For instance, as a previous study suggested, although temperature controls the processes of decomposition, nitrification, and denitrification, the ratio of N_2O to N_2 generally increases with decreasing temperature (Bouwman et al., 2002a). Furthermore, high N_2O emissions have even been observed in winter due to the accumulation of soil N in freeze–thaw cycles, despite the rather low temperatures (Kaiser and Ruser, 2000).

The heterogeneity of soil properties is also an important control on the variation in soil N_2O emissions. SOC and SN are important substrates for the soil microbial processes of nitrification and denitrification, while bulk density impacts the extent of anaerobic zones in the soil profile. Overall, correlation analyses suggest that precipitation, temperature, SOC, SN and bulk density are primarily responsible for interannual and inter-site variability in soil N_2O emissions. Further, the length of the experiment is an important factor which affects the quantification of N_2O emissions.

Based on our correlation analysis, we thus consider the following explanatory variables as the model inputs: *P*, SOC, SN, BD, and the length of experiments. As temperature has been recognized to be strongly related to soil processes associated with N_2O emissions (Bouwman et al., 2002a), we also consider temperature as input variable despite the weakly linear correlation. By applying the "holdout" method (Specht, 1991), we obtain the optimized spread parameter σ as 0.82. The GRNN is established to estimate N_2O emissions from natural soils with the spread parameter. The coefficient of determination (r^2) between the observed and simulated is 0.94 ($p < 0.01$). The simulated N_2O fluxes are close to the observed data (RMSE = 0.29 kg N ha^{-1}). The linear regression between the simulated and measured N_2O emissions is rather close to the 1:1 line (Fig. 2).

3.2. Global N_2O emissions

We estimate that the annual global N_2O emissions from soils under natural vegetation, encompassing an area of 92.34 million km^2, were 3.37 Tg N in year 2000. The simulated N_2O emission rates exhibit a large spatial variability (Fig. 3). The spatial patterns of the simulated emissions agree with previous studies by Potter et al. (1996) and Stehfest and Bouwman (2006), indicating that soil and climate characteristics are major factors. The simulated emission patterns show that the tropics are a predominant source of N_2O. The highest emissions occurred in the Amazon, Southeast Asia, and Central Africa. These regions generally receive a large amount of annual rainfall and are characterized by soils with high clay and organic carbon contents. Such conditions favor the microbial N turnover processes and consequently promote high N_2O production (Granli and Bockman, 1994). Lower N_2O emissions occurred in some temperate regions, such as East Asia, Europe, Australia, and North America. Some boreal regions, like south Russia and Canada, also exhibited relatively high N_2O emission rates, exceeding 0.20 kg N_2O–N ha^{-1} yr^{-1} due to high soil organic matter content and relatively moist climate. Stehfest and Bouwman (2006) also simulated a similar spatial pattern of N_2O emission rates ranging from 0 to 0.25 N_2O–N ha^{-1} yr^{-1} in the same regions. In contrast, the soils in the northern high latitudes and regions characterized by drought climate (e.g., Sahara and Arab) only contributed negligible emissions. The finding that N_2O emissions in tropical regions exceed those in the high latitudes and drought regions is in agreement with the literature, and suggests that thermal and hydrological regimes control soil processes at all levels by governing organic matter decomposition, nitrification and denitrification rates (Fig. 4; Bouwman et al., 2002a).

The spatial variation in soil N_2O emissions is attributed to the distribution of vegetation, in addition to the effects of climate and

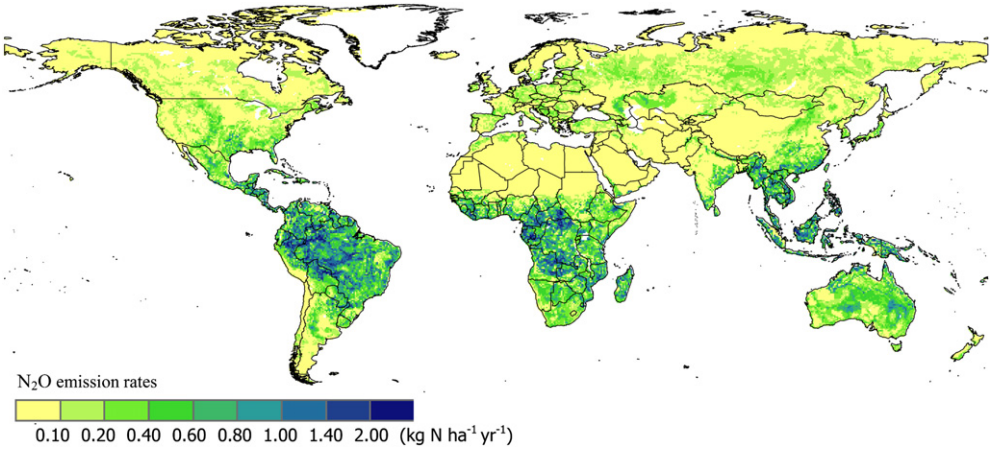

Fig. 3. Spatial patterns of soil N_2O emissions under natural vegetation in year 2000.

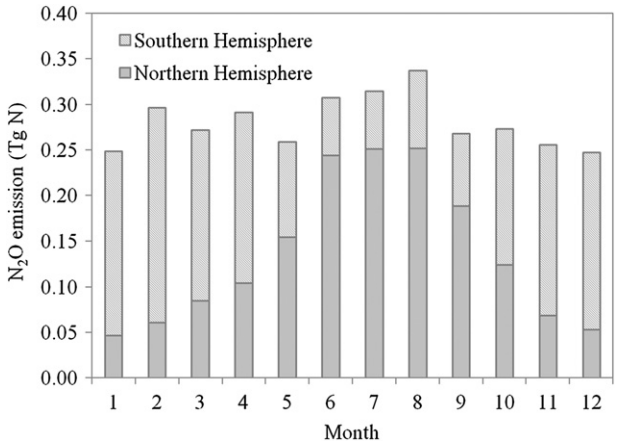

Fig. 4. Seasonal variation of soil N_2O emissions under natural vegetation.

soil type (Table 3). The N_2O source strength varied greatly across different types of natural ecosystems mainly due to their corresponding climate and soil conditions (Table 3). Among the natural ecosystems, the evergreen broadleaf forest areas are the most important sources of atmospheric N_2O, and accounts for 30% of the global annual N_2O emissions under natural vegetation (Table 2). On a per unit area basis, the evergreen broadleaf forest also shows the highest soil N_2O emissions at 0.81 kg N ha^{-1} yr^{-1}. As previously mentioned, tropical conditions and regions with high soil organic contents favor soil N_2O production and thus account for the high flux; this finding is also supported by the findings from field experiments and observations (e.g., Keller and Reiners, 1994; Breuer et al., 2000; Werner et al., 2007b). The woody savannas are the second largest emitter, accounting for 17% of the total emissions. Although the typical anoxic soils of wetlands are generally considered unfavorable for N_2O production, the total N_2O emissions from natural wetlands are still considerable (Blais et al., 2005; Dalal and Allen, 2008). Moreover, N_2O "hotspots" in sub-tropical wetlands suggest that the N_2O budget for wetlands should not be negligible (Corredor et al., 1999). Our results also indicated that wetlands are characterized as considerable N_2O emitters, with an annual rate of 0.36 kg N ha^{-1} yr^{-1} (Table 3). In contrast, as a result of low temperatures, the high latitude ecosystems, including evergreen needleleaf forests and deciduous needleleaf forests, have significantly low emission rates and contribute little to the global source (less than 0.10 Tg N per year). The intermediate emission rates and source strength occurred in the mixed forests, grasslands and shrublands.

N_2O emissions from soils under natural vegetation had significant seasonal variation in each hemisphere (Fig. 4). Emissions from the Northern Hemisphere exhibited one seasonal peak. The peak emissions occurred in August, while winters had low emissions. In contrast to the north, N_2O emissions changed in the opposite phase in the Southern Hemisphere. In spite of the contrasting patterns of seasonal emissions, the two hemispheres had almost equal source strengths for annual N_2O emissions at about 1.7 Tg N_2O–N yr^{-1}. Consequently, the total global N_2O emissions did not exhibit a significant seasonality, owing to this offsetting effect. The summer emissions were slightly higher than in other seasons.

Table 3
Estimates of soil N_2O emissions of different vegetation types in the year 2000.

Vegetation types	Area (million km^2)	N_2O source strength (Tg N yr^{-1})	N_2O flux (kg N ha^{-1} yr^{-1})
Evergreen needleleaf forest	4.07	0.05	0.11
Evergreen broadleaf forest	12.64	1.03	0.81
Deciduous needleleaf forest	1.42	0.02	0.12
Deciduous broadleaf forest	2.05	0.07	0.36
Mixed forests	5.85	0.13	0.22
Closed shrublands	2.34	0.06	0.27
Open shrublands	18.78	0.31	0.17
Woody savannas	14.20	0.59	0.42
Savannas	7.73	0.41	0.54
Grasslands	14.58	0.31	0.21
Wetlands	0.92	0.03	0.36
Vegetation mosaic	7.76	0.35	0.45
Total	92.34	3.37	0.36

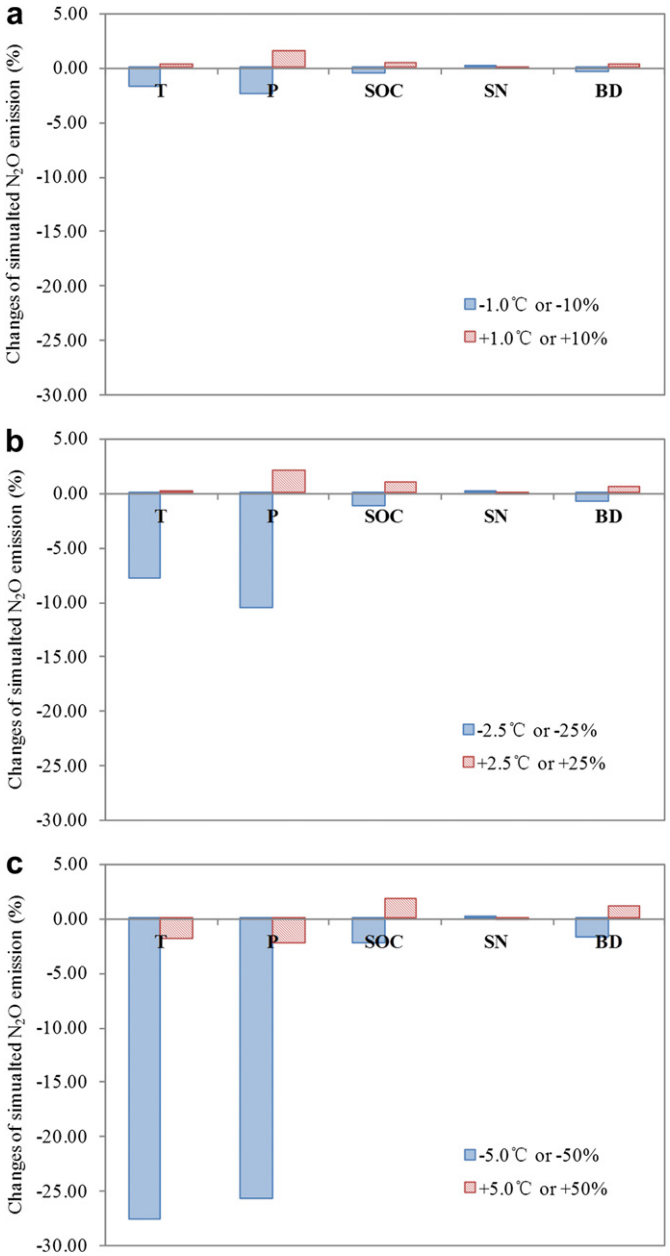

Fig. 5. Sensitivity studies of soil N_2O emissions under natural vegetation to changes in air temperature, precipitation, soil organic carbon, soil nitrogen content, and bulk density. The values are for the year 2000. The changes are calculated based on the "baseline" simulation using the unchanged global input data.

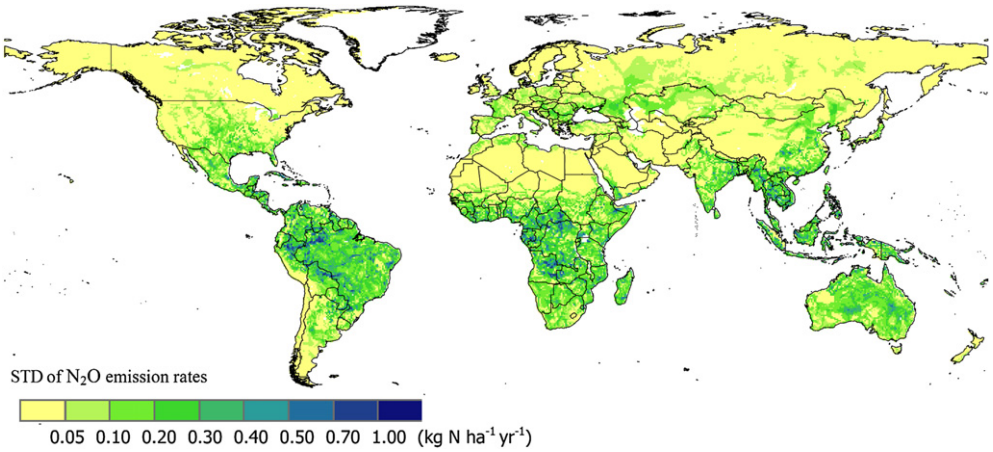

Fig. 6. Standard deviation (SD) of annual N_2O emission rates simulated with the one hundred ANN models.

3.3. Model sensitivity

By altering the input variables individually, we conduct a model sensitivity analysis (Fig. 5). The most sensitive input variable is precipitation. The pronounced sensitivity of the simulated N_2O emissions to changes in precipitation agrees with earlier studies, suggesting that the soil water conditions controls N_2O production through affecting nitrification and denitrification processes (Li et al., 2000). Further, N_2O emissions did not change uniformly with precipitation. "Large" increases in precipitation reduced N_2O emissions. This phenomenon agrees with experimental findings that suggest that precipitation reduces the production of N_2O in favor of denitrification to N_2 when soil moisture reaches a certain level (e.g., Conrad, 1996; Dobbie and Smith, 2003). Increasing temperature at a "small" level favors more global N_2O emissions than increasing temperatures at a "medium" level. The elevated temperature could lead to a substantial reduction in soil moisture due to increased transpiration. Thus, increasing temperature at a "large" level can have a reducing effect on N_2O emissions. Increasing soil organic carbon content and bulk density enhances N_2O emissions. In contrast, the global N_2O emissions were barely changed in response to alterations in soil nitrogen content (Fig. 5). The sensitivity of N_2O emissions to changes in SOC is a consequence of the dependency of microbial activity on the total available carbon fraction in soils. An increase in bulk density will decrease total pore volume, and thus oxygen diffusion into the soil profile. The increasing extent of anaerobic zones in the soil profile favors denitrification, and consequently promotes N_2O production. Overall, the availability of carbon, nitrate, and the oxygen supply are the most important factors controlling soil denitrification rates and N_2O production (Bouwman et al., 2002a). In general, the model is less sensitive to the changes in soil properties than to climate.

3.4. Uncertainty of the global inventory estimate

Based on one hundred ANN simulations, we find that a larger uncertainty usually accompanies a higher emission rate (Fig. 6). The estimates with different ANN models did not significantly differ at a grid cell level, as indicated by the standard deviations rarely exceeding 1.00 kg N ha^{-1} yr^{-1}. The one hundred ANN models provide a frequency distribution of the estimated global emissions (Fig. 7). We define the model-induced uncertainty of our global estimates as a range between the lower bound (1.96 Tg N yr^{-1}) and the upper bound (4.56 Tg N yr^{-1}) of the 95% confidence intervals, with a mean global estimate of 3.37 Tg N yr^{-1}.

Our estimates of global N_2O emissions are lower than other exiting estimates. For example, Potter et al. (1996) estimated that the global emissions from natural soil to be 6.1 Tg N yr^{-1} using a process-based model. Bouwman et al. (1995) estimated the emissions to be 6.6 Tg N yr^{-1} using a simple regression model with a range of 3.3–9.0 Tg N yr^{-1} Liu (1996) estimated the global background N_2O emissions to be 11.33 Tg N yr^{-1} based on DNDC (Li et al., 1992). Nevison et al. (1996) estimated the global N_2O emissions from both natural and managed soils to be 9.5 Tg N yr^{-1} using a nitrogen biosphere model. The mean annual global N_2O emissions estimated by Xu et al. (2008) for 1980–2000 were 13.31 Tg N yr^{-1} with a range of 8.19–18.43 Tg N yr^{-1} through a stoichiometric relationship of N_2O and CO_2 emissions from ecosystems, including cropland. Their simulated higher soil respiration of CO_2 may induce a higher N_2O estimate (Xu et al., 2008). The spatial patterns of our simulated emission rates agree with most previous studies (e.g., Liu, 1996; Potter et al., 1996; Werner et al., 2007a). Further, consistent with other studies (e.g., Matson and Vitousek, 1990; Bouwman et al., 1995; Stehfest and Bouwman, 2006), we confirm that tropical soils are a major source of atmospheric N_2O. Some studies have quantified N_2O emissions especially from the tropical ecosystems. For example, Melillo et al. (2001) estimated the emissions to be

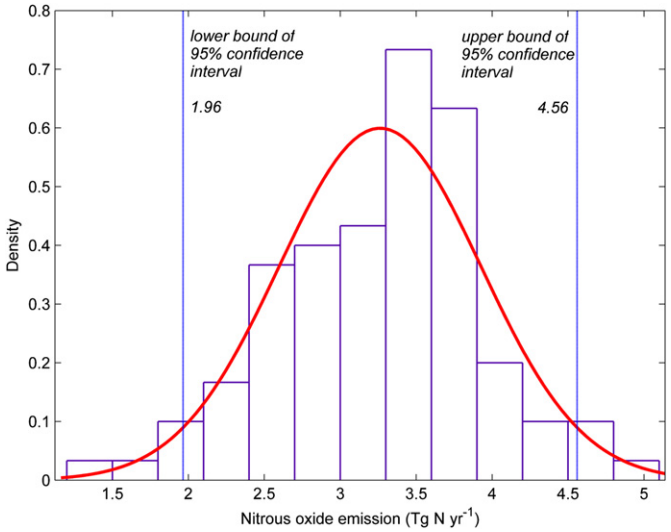

Fig. 7. Probability distribution and the 95% confidence intervals of the simulated annual global N_2O emissions with the one hundred ANN models.

1.3 Tg N yr^{-1} from tropical forests in the Amazon basin (5.4 million km^2), which is significantly higher than our estimate of 1.03 Tg N yr^{-1} for the global tropical forest. In their study, the soil N_2O emission is only determined by net nitrogen mineralization rates, rather than the multiple controlling factors considered in our study. Further, their estimates were calculated based on a loss rate of 1.4% for nitrogen mineralization. This static fraction may not be able to account for the heterogeneity of soil N_2O emissions in that large of an area. Stehfest and Bouwman (2006) estimated N_2O emissions from closed tropical forests to be 1.17 Tg N yr^{-1}, which is close to our calculation of 1.03 Tg N yr^{-1}. Recently, a detailed process-based biogeochemical model ForestDNDC-tropica was applied by Werner et al. (2007a) to determine the N_2O source strength of tropical rainforest ecosystems. Their estimates of 1.34 Tg N yr^{-1} for the total source strength are slightly higher than our estimates, but the vegetation category and the area extent of their calculation is also different from those used in our study.

A considerable uncertainty in developing the global inventory still exists. To reduce the uncertainty, more N_2O emission measurements and associated data for climate, soils, and vegetation, as well as finer-resolution spatial data are needed. The processes of nitrification and denitrification that determine the N cycling within ecosystems (e.g., N mineralization and N uptake by plants) and exchanges between ecosystems and the atmosphere (e.g., production and release of NO and N_2 in addition to N_2O) should be explicitly modeled.

4. Conclusions

Based on published N_2O emission measurements, we develop a model to estimate natural soil N_2O emissions using an artificial neural network approach. The ANN model fit well with observed N_2O emissions. We find that the annual global N_2O emissions are most sensitive to variations in precipitation. The model-induced uncertainty is assessed by developing one hundred alternative ANN models using different sample data. We estimate that the global soil N_2O source strength from natural ecosystems is on average 3.37 Tg N yr^{-1} with an uncertainty range of 1.96–4.56 Tg N yr^{-1} for the year 2000. The simulated N_2O emissions show a large spatial and seasonal variability due to variations in soil, vegetation, and climate conditions. Consistent with other studies, we confirm that tropical soils are the major source of atmospheric N_2O.

Acknowledgments

We thank Dr. E. Stefest and Dr. A.F. Bouwman to make their compiled N_2O emission and other ancillary data available to this analysis.

This study is supported by Department of Energy (DE-FG02-08ER64599), the NSF Division of Information & Intelligent Systems (IIS-1028291), the National Natural Science Foundation of China (NSFC, Grant No. 41105080), and the NSF Carbon and Water in the Earth Program (EAR-0630319). We thank Ms. Jayne Piepenburg for English editing. High performance computing is supported by the Rosen Center for Advanced Computing at Purdue University.

References

Anderson, I.C., Poth, M.A., 1989. Semiannual losses of nitrogen as NO and N_2O from unburned and burned chaparral. Global Biogeochemical Cycles 3 (2), 121–135.

Anghel, C., Ozunu, A., 2006. Prediction of gaseous emissions from industrial stacks using an artificial intelligence method. Chemical Papers 60, 410–415.

Batjes, N., 2006. ISRIC-WISE Derived Soil Properties on a 5 by 5 Arc-minutes Global Grid (Ver. 1.1). Report 2006/02. ISRIC - World Soil Information, Wageningen.

Blais, A.M., Lorrain, S., Tremblay, A., 2005. Greenhouse gas fluxes (CO_2, CH_4, and N_2O) in forests and wetlands of boreal, temperate and tropical regions. In: Greenhouse Gas Emissions - Fluxes and Process. Springer-Verlag, Berlin, Germany.

Bouwman, A.F., 1996. Direct emission of nitrous oxide from agricultural soils. Nutrient Cycling in Agroecosystems 46, 53–70.

Bouwman, A.F., Boumans, L.J.M., Batjes, N.H., 2002a. Emissions of N_2O and NO from fertilized fields: summary of available measurement data. Global Biogeochemical Cycles 16, 1058.

Bouwman, A.F., Boumans, L.J.M., Batjes, N.H., 2002b. Modeling global annual N_2O and NO emissions from fertilized fields. Global Biogeochemical Cycles 16, 1080.

Bouwman, A.F., Van der Hoek, K.W., Olivier, J.G.J., 1995. Uncertainties in the global source distribution of nitrous oxide. Journal of Geophysical Research 100, 2785–2800.

Bowden, R.D., Steudler, P.A., Melillo, J.M., 1990. Annual nitrous oxide fluxes from temperate forest soils in the northeastern United States. Journal of Geophysical Research 96 (D9), 13997–14005.

Breuer, L., Papen, H., Butterbach-Bahl, K., 2000. N_2O emission from tropical forest soils of Australia. Journal of Geophysical Research 105, 26353–26367.

Butterbach-Bahl, K., Gasche, R., Huber, C., Kreutzer, K., Papen, H., 1998. Impact of N-input by wet deposition on N-trace gas fluxes and CH4-oxidation in spruce forest ecosystems of the temperate zone in Europe. Atmospheric Environment 32 (3), 559–564.

Butterbach-Bahl, K., Gasche, R., Breuer, L., Papen, H., 1997. Fluxes of NO and N_2O from temperate forest soils: impact of forest type, N deposition and of liming on the NO and N_2O emissions. Nutrient Cycling in Agroecosystems 48 (1), 79–90.

Butterbach-Bahl, K., Kahl, M., Mykhayliv, K., Werner, C., Kiese, R., Li, C., 2009. A European-wide inventory of soil NO emissions using the biogeochemical models DNDC/Forest-DNDC. Atmospheric Environment 43 (7), 1392–1402.

Castro, M.S., Steudler, P.A., Melillo, J.M., Aber, J.D., Millham, S., 1992. Exchange of N_2O and CH_4 between the atmosphere and soils in spruce-fir forests in the northeastern United States. Biogeochemistry 18 (3), 119–135.

Cates, R.L., Keeney, D.R., 1987. Nitrous oxide production throughout the year from fertilized and manured maize fields. Journal of Environmental Quality 16 (4), 443–447.

Cigizoglu, H.K., Alp, M., 2006. Generalized regression neural network in modelling river sediment yield. Advances in Engineering Software. ISSN: 0965-9978 37 (2). ISSN: 0965-9978, 63–68. doi:10.1016/j.advengsoft.2005.05.002.

Conrad, R., 1996. Soil microorganisms as controllers of atmospheric trace gases (H_2, CO, CH_4, OCS, N_2O, and NO). Microbiology and Molecular Biology Reviews 60, 609–640.

Corredor, J.E., Morell, J.M., Bauza, J., 1999. Atmospheric nitrous oxide fluxes from mangrove sediments. Marine Pollution Bulletin 38, 473–478.

Dalal, R.C., Allen, D.E., 2008. TURNER REVIEW No. 18. Greenhouse gas fluxes from natural ecosystems. Australian Journal of Botany 56, 369–407.

Delon, C., Serça, D., Boissar, C., Dupont, R., Dutot, A., Laville, P., De Rosnay, P., Delmas, R., 2007. Soil NO emissions modelling using artificial neural network. Tellus B 59, 502–513.

Disorntetiwat, P., Dagli, C.H., 2000. Simple ensemble-averaging model based on generalized regression neural network in financial forecasting problems. In: Adaptive Systems for Signal Processing, Communications, and Control Symposium 2000, AS-SPCC. The IEEE 2000, pp. 477–480.

Dobbie, K.E., Smith, K.A., 2003. Nitrous oxide emission factors for agricultural soils in Great Britain: the impact of soil water-filled pore space and other controlling variables. Global Change Biology 9, 204–218.

Dupont, R., Butterbach-Bahl, K., Delon, C., Bruggemann, N., Serca, D., 2008. Neural network treatment of 4 years long NO measurement in temperate spruce and beech forests. Journal of Geophysical Research 113, G04001.

Duxbury, J.M., Bouldin, D.R., Terry, R.E., Tate, R.L., 1982. Emissions of nitrous oxide from soils. Nature 298, 462–464.

Erickson, H., Davidson, E.A., Keller, M., 2002. Former land-use and tree species affect nitrogen oxide emissions from a tropical dry forest. Oecologia 130 (2), 297–308.

Flynn, H.C., Smith, J., Smith, K.A., Wright, J., Smith, P., Massheder, J., 2005. Climate- and crop-responsive emission factors significantly alter estimates of current and future nitrous oxide emissions from fertilizer use. Global Change Biology 11, 1522–1536.

Garcia-Montiel, D.C., Steudler, P.A., Piccolo, M., Neill, C., Melillo, J., Cerri, C.C., 2003. Nitrogen oxide emissions following wetting of dry soils in forest and pastures in Rondônia, Brazil. Biogeochemistry 64, 319–336.

Goodroad, L.L., Keeney, D.R., 1984. Nitrous oxide production in aerobic soils under varying pH, temperature and water content. Soil Biology & Biochemistry 16, 39–43.

Goossens, A., Visscher, A.D., Boeckx, P., Van Cleemput, O., 2001. Two-year field study on the emission of N_2O from coarse and middle-textured Belgian soils with different land use. Nutrient Cycling in Agroecosystems 60 (1), 23–34.

Granli, T., Bockman, O.C., 1994. Nitrogen oxide from agriculture. Norwegian Journal of Agricultural Sciences 12, 7–127.

Hao, W.M., Scharffe, D., Crutzen, P.J., Sanhueza, E., 1988. Production of N_2O, CH_4, and CO_2 from soils in the tropical savanna during the dry season. Journal of Atmospheric Chemistry 7 (1), 93–105.

Horwath, W.R., Elliott, L.F., Steiner, J.J., Davis, J.H., Griffith, S.M., 1998. Denitrification in cultivated and noncultivated riparian areas of grass cropping systems. Journal of Environmental Quality 27 (4), 225–231.

Intergovermental Panel on Climate Change (IPCC), 2007. Climate change 2007: the physical science basis. In: Solomon, S., et al. (Eds.), Working Group I Contribution

to the Fourth Assessment Report of the Intergovernmental Panel on Climate Change, Cambridge, United Kingdom and New York, NY, USA.
Ishizuka, S., Tsuruta, H., Murdiyarso, D., 2002. An intensive field study on CO_2, CH_4, and N_2O emissions from soils at four land-use types in Sumatra, Indonesia. Global Biogeochemical Cycles 16, 1049. doi:10.1029/2001GB001614.
Kaiser, E.A., Ruser, R., 2000. Nitrous oxide emissions from arable soils in Germany: an evaluation of six long-term field experiments. Journal of Plant Nutrition and Soil 163, 249–259.
Keller, M., Goreau, T.J., Wofsy, S.C., Kaplan, W.A., McElroy, M.B., 1983. Production of nitrous oxide and consumption of methane by forest soils. Geophysical Research Letters 10 (2), 1156–1159.
Keller, M., Kaplan, W.A., Wofsy, S.C., 1986. Emissions of N_2O, CH_4, and CO_2 from tropical forest soils. Journal of Geophysical Research 91 (D11), 11791–11802.
Keller, M., Kaplan, W.A., Wofsy, S.C., Dacosta, J.M., 1988. Emissions of N_2O from tropical forest soils: response to fertilization with NH_4^+, NO_3^-, and PO_4^{3-}. Journal of Geophysical Research-Atmospheres 93 (D2), 1600–1604.
Keller, M., Reiners, W.A., 1994. Soil-atmosphere exchange of nitrous oxide, nitric oxide, and methane under secondary succession of pasture to forest in the Atlantic lowlands of Costa Rica. Global Biogeochemical Cycles 8, 399–409.
Kiese, R., Butterbach-Bahl, K., 2002. N_2O and CO_2 emissions from three different tropical forest sites in the wet tropics of Queensland, Australia. Soil Biology & Biochemistry 34, 975–987.
Levine, J.S., Winstead, E.L., Parsons, D.A.B., Scholes, M.C., Scholes, R.J., Cofer III, W.R., Cahoon Jr., D.R., Sebacher, D.I., 1996. Biogenic soil emissions of nitric oxide (NO) and nitrous oxide (N_2O) from savannas in South Africa: the impact of wetting and burning. Journal of Geophysical Research 101 (D19), 23689–23697.
Li, C., Aber, J., Stange, F., Butterbach-Bahl, K., Papen, H., 2000. A process-oriented model of N_2O and NO emissions from forest soils: 1. Model development. Journal of Geophysical Research 105, 4369–4384.
Li, C., Frolking, S., Frolking, T.A., 1992. A model of nitrous oxide evolution from soil driven by rainfall events: 1. Model structure and sensitivity. Journal of Geophysical Research 97, 9759–9776.
Liu, Y., 1996. Modeling the Emissions of Nitrous Oxide (N_2O) and Methane (CH_4) from the Terrestrial Biosphere to the Atmosphere. Massachusetts Institute of Technology.
Lu, Y., Huang, Y., Zou, J., Zheng, X., 2006. An inventory of N_2O emissions from agriculture in China using precipitation-rectified emission factor and background emission. Chemosphere 65, 1915–1924.
Luizão, F., Matson, P., Livingston, G., Luizão, R., Vitousek, P., 1989. Nitrous oxide flux following tropical land clearing. Global Biogeochemical Cycles 3 (3), 281–285. doi:10.1029/GB003i003p00281.
Matson, P.A., Vitousek, P.M., 1987. Cross-system comparisons of soil nitrogen transformations and nitrous oxide flux in tropical forest ecosystems. Global Biogeochemical Cycles 1 (2), 163–170. doi:10.1029/GB001i002p00163.
Matson, P.A., Vitousek, P.M., 1990. Ecosystem approach to a global nitrous oxide budget. BioScience 40, 667–672.
Matson, P.A., Vitousek, P.M., Livingston, G.P., Swanberg, N.A., 1990. Sources of variation in nitrous oxide flux from Amazonian ecosystems. Journal of Geophysical Research 95 (D10), 16789–16798. doi:10.1029/JD095iD10p16789.
Melillo, J.M., Steudler, P.A., Feigl, B.J., Neill, C., Garcia, D., Piccolo, M.C., Cerri, C.C., Tian, H., 2001. Nitrous oxide emissions from forests and pastures of various ages in the Brazilian Amazon. Journal of Geophysical Research 106 (D24), 34179–34188.
Mitchell, T.D., Jones, P.D., 2005. An improved method of constructing a database of monthly climate observations and associated high-resolution grids. International Journal of Climatology 25, 693–712.
Mo, J.M., Fang, Y.T., Lin, E.D., Li, Y.E., 2006. Soil N_2O emission and its response to simulated N deposition in the main forests of DinHuShan in subtropical China. Chinese Journal of Plant Ecology 30, 901–910.
Mogge, B., Kaiser, E.A., Munch, J.C., 1998. Nitrous oxide emissions and denitrification N-losses from forest soils in the Bornhöved lake region (Northern Germany). Soil Biology & Biochemistry 30 (6), 703–710.
Mosier, A.R., Stillwell, M., Parton, W.J., Woodmansee, R.G., 1981. Nitrous oxide emissions from a native shortgrass prairie. Soil Science Society of America Journal 45, 617–619.
Mummey, D.L., Smith, J.L., Bolton Jr., H., 1997. Small-scale spatial and temporal variability of N_2O flux from a shrub-steppe ecosystem. Soil Biology & Biochemistry 29 (11), 1699–1706.
Nevison, C.D., Esser, G., Holland, E.A., 1996. A global model of changing N_2O emissions from natural and perturbed soils. Climatic Change 32, 327–378.
Palm, C.A., Alegre, J.C., Arevalo, L., Mutuo, P.K., Mosier, A.R., Coe, R., 2002. Nitrous oxide and methane fluxes in six different land use systems in the Peruvian Amazon. Global Biogeochemical Cycles 16 (4), 1073. doi:10.1029/2001GB001855.
Parton, W.J., Mosier, A.R., Schimel, D.S., 1988. Rates and pathways of nitrous oxide production in a shortgrass steppe. Biogeochemistry 6 (1), 45–58.
Parton, W.J., Mosier, A.R., Ojima, D.S., Valentine, D.W., Schimel, D.S., Weier, K., Kulmala, A.E., 1996. Generalized model for N_2 and N_2O production from nitrification and denitrification. Global Biogeochemical Cycles 10, 401–412.
Pitcairn, C.E.R., Skibaa, U.M., Suttona, M.A., Fowlera, D., Munroa, R., Kennedy, V., 2002. Defining the spatial impacts of poultry farm ammonia emissions on species composition of adjacent woodland groundflora using Ellenberg Nitrogen Index, nitrous oxide and nitric oxide emissions and foliar nitrogen as marker variables. Environmental Pollution 119 (1), 9–21.
Poth, M., Anderson, I.C., Miranda, H.S., Miranda, A.C., Riggan, P.J., 1995. The magnitude and persistence of soil NO, N_2O, CH_4, and CO_2 fluxes from burned tropical savanna in Brazil. Global Biogeochemical Cycles 9 (4), 503–513. doi:10.1029/95GB02086.
Potter, C.S., Matson, P.A., Vitousek, P.M., Davidson, E.A., 1996. Process modeling of controls on nitrogen trace gas emissions from soils worldwide. Journal of Geophysical Research 101, 1361–1377.
Riley, R.H., Vitousek, P.M., 1995. Nutrient dynamics and nitrogen trace gas flux during ecosystem development in montane rainforest. Ecology 76 (1), 292–304.
Sanhueza, E., Hao, W.M., Scharffe, D., Donoso, L., Crutzen, P.J., 1990. N_2O and NO emissions from soils of the northern part of the Guayana Shield, Venezuela. Journal of Geophysical Research 95 (D13), 22481–22488. doi:10.1029/JD095iD13p22481.
Sanhueza, E., Cardenas, L., Donoso, L., Santana, M., 1994. Effect of plowing on CO_2, CO, CH_4, N_2O and NO fluxes from tropical savannah soils. Journal of Geophysical Research 99D, 16429–16434.
Schmidt, J., Seiler, W., Conrad, R., 1988. Emission of nitrous oxide from temperate forest soils into the atmosphere. Journal of Atmospheric Chemistry 6 (1), 95–115.
Scholes, M.C., Martin, R., Scholes, R.J., Parsons, D., Winstead, E., 1997. NO and N_2O emissions from savanna soils following the first simulated rains of the season. Nutrient Cycling in Agroecosystems 48, 115–122. doi:10.1023/a:1009781420199.
Seiler, W., Conrad, R., 1981. Field measurements of natural and fertilizer-induced N_2O release rates from soils. Journal of the Air Pollution Control Association 31 (7), 767–772.
Serca, D., Delmas, R., Jambert, C., Labroue, L., 1994. Emissions of nitrogen oxides from equatorial Rainforest in central Africa. Tellus B 46 (4), 243–254.
Skiba, U.M., Fowler, D., Smith, K.A., 1997. Nitric oxide emissions from agricultural soils in temperate and tropical climates: sources, controls and mitigation options. Nutrient Cycling in Agroecosystems 48 (1), 139–153.
Skiba, U.M., Sheppard, L.J., Pitcairn, C.E.R., Van Duk, S., Rossall, M.J., 1999. The effect of N deposition on nitrous oxide and nitric oxide emissions from temperate forest soils. Water, Air, & Soil Pollution 116 (1), 89–98.
Skiba, U.M., Sheppard, L.J., MacDonald, J., Fowler, D., 1998. Some key environmental variables controlling nitrous oxide emissions from agricultural and semi-natural soils in Scotland. Atmospheric Environment 32 (19), 3311–3320.
Skiba, U., Smith, K.A., 2000. The control of nitrous oxide emissions from agricultural and natural soils. Chemosphere - Global Change Science 2, 379–386.
Smith, C.J., DeLaune, R.D., Patrick Jr., W.H., 1983. Nitrous oxide emission from Gulf Coast wetlands. Geochimica et Cosmochimica Acta 47 (10), 1805–1814.
Smith, K.A., Conen, F., 2004. Impacts of land management on fluxes of trace greenhouse gases. Soil Use and Management 20, 255–263.
Specht, D.F., 1991. A general regression neural network. Neural Networks, Institute of Electrical and Electronics Engineers (IEEE) Transactions 2, 568–576.
Stehfest, E., Bouwman, L., 2006. N_2O and NO emission from agricultural fields and soils under natural vegetation: summarizing available measurement data and modeling of global annual emissions. Nutrient Cycling in Agroecosystems 74, 207–228.
Steudler, P.A., Garcia-Montiel, D.C., Piccolo, M.C., Neill, C., Melillo, J.M., Feigl, B.J., Cerri, C.C., 2002. Trace gas responses of tropical forest and pasture soils to N and P fertilization. Global Biogeochemical Cycles 16 (2), 1023. doi:10.1029/2001GB001394.
Verchot, L.V., Hutabarat, L., Hairiah, K., van Noordwijk, M., 2006. Nitrogen availability and soil N_2O emissions following conversion of forests to coffee in southern Sumatra. Global Biogeochemical Cycles 20, GB4008. doi:10.1029/2005GB002469.
Vitousek, P., Matson, P., Volkmann, C., Maass, J.M., Garcia, G., 1989. Nitrous oxide flux from dry tropical forests. Global Biogeochemical Cycles 3 (4), 375–382. doi:10.1029/GB003i004p00375.
Wang, Y.F., Ma, X.Z., Ji, B.M., Du, R., Chen, Z.Z., Wang, G.C., Wang, Y.S., Wan, X.W., 2003. Diurnal and seasonal variation in methane and nitrous oxide fluxes in meadow steppe of Inner Mongolia. Chinese Journal of Plant Ecology 27, 792–797.
Werner, C., Butterbach-Bahl, K., Haas, E., Hickler, T., Kiese, R., 2007a. A global inventory of N_2O emissions from tropical rainforest soils using a detailed biogeochemical model. Global Biogeochemical Cycles 21, GB3010.
Werner, C., Kiese, R., Butterbach-Bahl, K., 2007b. Soil-atmosphere exchange of N_2O, CH_4, and CO_2 and controlling environmental factors for tropical rain forest sites in western Kenya. Journal of Geophysical Research 112, D03308.
Weitz, A.M., Veldkamp, E., Keller, M., Neff, J., Crill, P.M., 1998. Nitrous oxide, nitric oxide, and methane fluxes from soils following clearing and burning of tropical secondary forest. Journal of Geophysical Research 103 (D21), 28047–28058. doi:10.1029/98JD02144.
Xu, X., Tian, H., Hui, D., 2008. Convergence in the relationship of CO_2 and N_2O exchanges between soil and atmosphere within terrestrial ecosystems. Global Change Biology 14, 1651–1660.
Zhuang, Q., Zhang, T., Xiao, J., Luo, T., 2008. Quantification of net primary production of Chinese forest ecosystems with spatial statistical approaches. Mitigation and Adaptation Strategies for Global Change. doi:10.1007/s11027-008-9152-7.